

ERK activation and autophagy impairment are central mediators of irinotecan-induced steatohepatitis

Abdo Mahli,^{1,2} Michael Saugspier,¹ Andreas Koch,^{1,2} Judith Sommer,^{1,2} Peter Dietrich,² Seren Lee,³ Reinhard Thasler,³ Jan Schulze-Luehrmann,⁴ Anja Luehrmann,⁴ Wolfgang Erwin Thasler,³ Martina Müller,¹ Anja Bosserhoff,^{2,5} Claus Hellerbrand^{1,2}

► Additional material is published online only. To view please visit the journal online (<http://dx.doi.org/10.1136/gutjnl-2016-312485>).

¹Department of Internal Medicine I, University Hospital Regensburg, Regensburg, Germany

²Institute of Biochemistry (Emil-Fischer Zentrum), Friedrich-Alexander University Erlangen-Nürnberg, Erlangen, Germany

³Biobank o.b. HTCR, Department of General Visceral- and Transplantation Surgery, Ludwig-Maximilians-University Munich, Munich, Germany

⁴Mikrobiologisches Institut – Klinische Mikrobiologie, Immunologie und Hygiene, Universitätsklinikum Erlangen, Friedrich-Alexander-Universität (FAU) Erlangen-Nürnberg, Erlangen, Germany

⁵Comprehensive Cancer Center Erlangen, CCC Erlangen-EMN, Erlangen, Germany

Correspondence to

Professor Claus Hellerbrand, Institute of Biochemistry, Friedrich-Alexander University Erlangen-Nürnberg, Erlangen D-91054, Germany; claus.hellerbrand@fau.de

Received 22 June 2016

Revised 7 December 2016

Accepted 8 December 2016

Published Online First

4 January 2017

ABSTRACT

Objective Preoperative chemotherapy with irinotecan is associated with the development of steatohepatitis, which increases the risk of perioperative morbidity and mortality for liver surgery. The molecular mechanisms of this chemotherapeutic complication are widely unknown.

Design Mechanisms of irinotecan-induced steatohepatitis were studied in primary human hepatocytes in vitro, in mice treated with irinotecan and in liver specimens from irinotecan-treated compared with control patients.

Results Irinotecan dose-dependently induced lipid accumulation and pro-inflammatory gene expression in hepatocytes. This was accompanied by an impairment of mitochondrial function with reduced expression of carnitine palmitoyltransferase I and an induction of acyl-coenzyme A oxidase-1 (ACOX1), oxidative stress and extracellular signal-regulated kinase (ERK) activation. ERK inhibition prevented irinotecan-induced pro-inflammatory gene expression but had only a slight effect on lipid accumulation. However, irinotecan also induced an impairment of the autophagic flux mediated by alkalisation of lysosomal pH. Re-acidification of lysosomal pH abolished irinotecan-induced autophagy impairment and lipid accumulation. Also in mice, irinotecan treatment induced hepatic ACOX1 expression, ERK phosphorylation and inflammation, as well as impairment of autophagy and significant steatosis. Furthermore, irinotecan-treated patients revealed higher hepatic ERK activity, expression of pro-inflammatory genes and markers indicative for a shift to peroxisomal fatty acid oxidation and an impaired autophagic flux. Pretreatment with the multityrosine kinase inhibitor sorafenib did not affect autophagy impairment and steatosis but significantly reduced ERK phosphorylation and inflammatory response in irinotecan-treated hepatocytes and murine livers.

Conclusions Irinotecan induces hepatic steatosis via autophagy impairment and inflammation via ERK activation. Sorafenib appears as a novel therapeutic option for the prevention and treatment of irinotecan-induced inflammation.

INTRODUCTION

The topoisomerase 1 inhibitor irinotecan (CPT-11) is a semisynthetic derivative of camptothecin, an

Significance of this study

What is already known on this subject?

- Neoadjuvant chemotherapy is increasingly being used to enlarge the cohort of patients who can be offered hepatic resection for malignancy.
- Inclusion of irinotecan in preoperative chemotherapy regimens is associated with the risk to develop steatohepatitis in a significant number of cases.
- Irinotecan-induced steatohepatitis is associated with an increased morbidity and mortality following hepatic resection.
- The multityrosine kinase inhibitor sorafenib augments the antitumour efficacy of irinotecan and overcomes irinotecan resistance in GI malignancies.

What are the new findings?

- Irinotecan induces extracellular signal-regulated kinase (ERK) activation in hepatocytes and murine and human liver tissue.
- Irinotecan alkalises the lysosomal pH in hepatocytes and herewith impairs the autophagic flux and causes cellular lipid accumulation.
- Specific ERK inhibition as well as sorafenib treatment prevented irinotecan-induced inflammation in hepatocytes and murine livers.

How might it impact on clinical practice in the foreseeable future?

- Sorafenib may be used for the prevention and treatment of irinotecan-induced (steato) hepatitis and may potentially improve irinotecan efficacy.

alkaloid extracted from the Chinese plant *Camptotheca acuminata*, and a very active antineoplastic drug for a number of cancer entities. It is also increasingly used in perioperative chemotherapy regimens to enlarge the number of patients who can be offered hepatic resection for colorectal liver metastases by downsizing hepatic tumour



To cite: Mahli A, Saugspier M, Koch A, et al. *Gut* 2018;**67**:746–756.

load.¹ However, there is increasing awareness of irinotecan-induced hepatotoxicity and its effect on outcome after hepatic resection.² Several observational clinical studies have reported that the inclusion of irinotecan in preoperative chemotherapy regimens is associated with the risk to develop steatohepatitis in up to 50% of cases.³ Furthermore, there is significant evidence that the presence of chemotherapy-induced steatohepatitis is associated with an increased morbidity and possibly mortality following hepatic resection as a result of hepatic insufficiency.^{3–5}

Despite the clinical implications of irinotecan-induced steatohepatitis, the underlying molecular mechanisms are widely unknown and there are no therapeutic strategies to prevent or treat this chemotherapeutic complication. In this study, we analysed the effect of irinotecan in primary human hepatocytes (PHH) and mice and uncovered that hepatocellular steatosis and inflammation are induced via impairment of different cellular organelles and mechanisms, respectively. Results have been verified in liver specimens from irinotecan-treated patients. Moreover, we analysed the effect of combined treatment of irinotecan with sorafenib and discovered a so far unknown effect of this multityrosine kinase inhibitor; sorafenib was able to inhibit irinotecan-induced inflammation in hepatocytes and murine livers.

MATERIALS AND METHODS

Cells and cell culture

Isolation and culture of PHH were performed as described.^{6,7} Furthermore, we used HepG2 cells (ATCC HB-8065) to establish experimental conditions for *in vitro* treatment with irinotecan. In diverse experiments, irinotecan treatment was performed in combination with N-acetylcysteine (NAC; 0.4 mM), a specific extracellular signal-regulated kinase (ERK) inhibitor (U0126; 10 μ M), a specific p38 inhibitor (SB202190; 10 μ M), chloroquine (CQ; 10 μ M), clioquinol (CLQ; 10 μ M) or sorafenib (BAY 43-9006; 0.5–4 μ M).

Murine models of irinotecan-induced steatohepatitis

Ten-week-old female C57BL/6 mice were obtained from Charles River Laboratories (Sulzfeld, Germany). Mice were maintained in specific pathogen-free housing and animal experiments were performed according to national and international guidelines of the European Union. After 2 weeks of acclimatization, mice were treated with intraperitoneal injections of irinotecan (50 mg/kg) or solvent (saline) every three days for 2 weeks (n=10 mice/group). This irinotecan dose has been used before to study antitumorigenic effects in murine cancer models.⁸ Twelve hours after the last injection, mice were killed and liver tissue and blood samples were collected for further analysis. In a second set of experiments, mice were treated with a single dose of irinotecan (50 mg/kg) alone or in combination with sorafenib (10 or 20 mg/kg) and sacrificed 24 hours thereafter. Mice injected with solvent served as controls.

Human liver tissues

Liver specimens of patients with metastatic colorectal cancer (i) with irinotecan treatment (n=6) or (ii) without chemotherapy (n=5) were obtained during resection of liver metastases, immediately snap frozen and stored at -80°C . Human liver tissues were obtained and experimental procedures were performed according to the guidelines of the charitable state-controlled foundation Human Tissue and Cell Research,⁹ with the informed patients' consent.

Statistical analysis

Results are expressed as mean \pm SEM. Comparisons between groups were performed using the unpaired Student's t-test or one-way analysis of variance, if appropriate. A p value<0.05 was considered statistically significant. All calculations were carried out using the statistical computer package GraphPad Prism V4.00 for Windows (GraphPad Software, San Diego, USA).

Additional methods

Detailed methodology is described in the 'Methods' section of the online supporting information.

RESULTS

Effect of irinotecan on hepatocellular steatosis *in vitro*

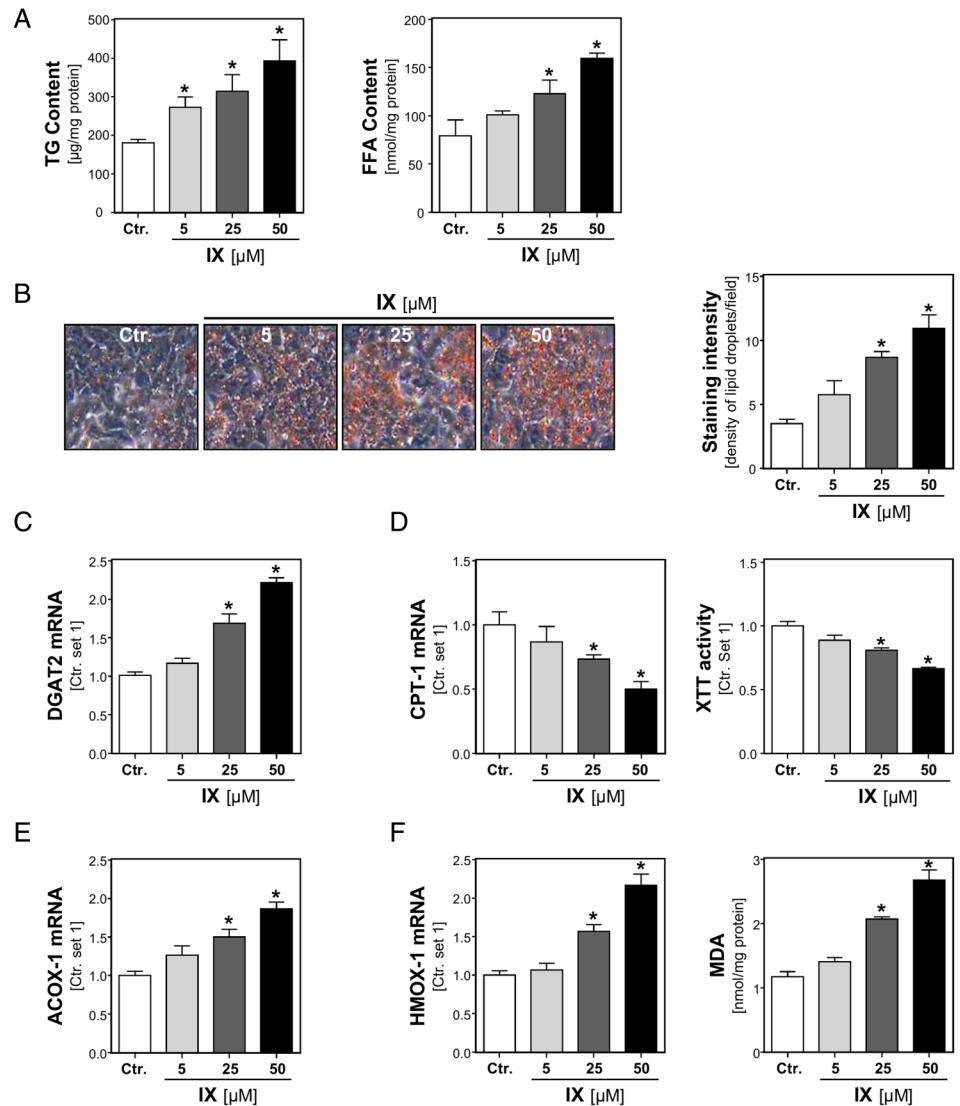
Initially, the dose range in which irinotecan did not affect viability of human hepatocytes was determined. Concentrations up to 50 μ M irinotecan did not cause toxic effects in PHH as well as in HepG2 cells (see online supplementary figure S1A,B) but dose-dependently increased cellular free fatty acid (FFA) and triglyceride (TG) levels (figure 1A). Oil red O staining confirmed an accumulation of small lipid droplets in irinotecan-treated cells (figure 1B). In line with these results, expression levels of diglyceride acyltransferase 2 (DGAT2), which catalyses the terminal step in the formation of TGs, were dose-dependently increased by irinotecan (figure 1C). This increase in lipid content appeared to be independent of *de novo* lipogenesis because irinotecan induced a significant downregulation of fatty acid synthase gene expression, the key enzyme of the *de novo* lipogenesis pathway (see online supplementary figure S1C). Despite cellular lipid accumulation, irinotecan reduced expression of carnitine palmitoyltransferase I (CPT-1), the key enzyme of the mitochondrial β -oxidation (figure 1D), and XTT activity, an indicator of mitochondrial activity (figure 1D). In contrast, irinotecan induced the expression of acyl-coenzyme A oxidase 1 (ACOX1) (figure 1E), indicative for an activation of the extra-mitochondrial fatty acid oxidation system in peroxisomes, which is known to lead to enhanced production of reactive oxygen species (ROS).¹⁰ In line with this, irinotecan treatment caused a marked increase of haem oxygenase-1 (HMOX-1) expression and malondialdehyde (MDA) levels as markers for oxidative stress (figure 1F).

Effect of irinotecan on hepatocellular ERK and p38 activation and pro-inflammatory gene expression *in vitro*

Oxidative stress is a known inducer of mitogen-activated protein kinases (MAPK) and pro-inflammatory gene expression. Irinotecan dose-dependently induced phosphorylation of ERK and p38 (figure 2A) as well as expression of interleukin-8 (IL-8), intercellular adhesion molecule 1 (ICAM-1) (figure 2B) and C-C motif chemokine ligand 5 (CCL5; RANTES) (see online supplementary figure S2A). The expression of these pro-inflammatory genes is known to correlate with hepatic inflammation in non-alcoholic fatty liver disease.^{11–13}

These effects were inhibited by preincubation with the ROS scavenger NAC (figure 2C, D and online supplementary figure S2B), confirming that oxidative stress is responsible for the observed irinotecan effects on MAPK activation and pro-inflammatory gene expression. Moreover, inhibition of the ERK pathway using a specific inhibitor (U0126) ameliorated irinotecan-induced IL-8, ICAM-1 and CCL5 expression (figure 2E and online supplementary figure S2C). In contrast, a specific inhibitor of p38 (SB202190) did not affect the expression of these genes (figure 2E and online supplementary figure S2C).

Figure 1 Effect of irinotecan (IX) on hepatocellular lipid accumulation and combustion in vitro. (A) Analysis of cellular triglyceride (TG) and free fatty acid (FFA) content normalised to total cellular protein in control (Ctr.) and irinotecan (IX)-treated hepatocytes. (B) Microscopic images (left panel) and quantification of staining intensity (right panel) of Oil red O staining. (C) Analysis of diglyceride acyltransferase 2 (DGAT2) mRNA expression by quantitative real time-PCR. (D) Carnitine palmitoyltransferase I (CPT-1) mRNA levels (left panel) and XTT activity (right panel). (E) Acyl-coenzyme A oxidase-1 (ACOX-1) mRNA levels. (F) Haem oxygenase-1 (HMOX1) mRNA levels (left panel) and cellular malondialdehyde (MDA) levels (right panel) (* $p < 0.05$ compared with control).



However, SB202190 slightly inhibited irinotecan-induced TG accumulation in hepatocytes while ERK inhibition had no effects on cellular steatosis (figure 2F).

Effect of irinotecan on lysosomal pH and autophagy in vitro

Activation of p38 has been shown to inhibit autophagy,^{14 15} and impaired autophagy is increasingly recognised as a critical factor in the pathogenesis of alcoholic and non-alcoholic fatty liver disease.^{16 17} Therefore, we investigated the effect of irinotecan on the cleavage of the microtubule-associated 1 light chain 3 (LC3). The lipidation of LC3-I with phosphatidylethanolamine leads to the formation of LC3-II, which is a critical step in autophagosome formation. Surprisingly, irinotecan treatment of hepatocytes increased the LC3-II/LC3-I ratio in a dose-dependent manner (figure 3A). However, irinotecan also caused elevated levels of sequestome 1 (p62), a protein that is degraded by autophagy and accumulates when autophagy is impaired. This suggested that the increase in LC3-II levels was not caused by an enhanced formation but rather an impaired clearance of autophagosomes. Fitting to this, LC3 staining showed accumulation of LC3 fluorescent puncta in the cytosol (figure 3B). A critical step of autophagy is the fusion of the autophagosome with a lysosome leading to the degradation and recycling of its content. For the activity of lysosomal enzymes, a low pH in the

lysosome is required.¹⁸ Interestingly, ratiometric pH measurements with LysoSensor Yellow/Blue DND-160 revealed that irinotecan markedly elevated the lysosomal pH in hepatocytes (figure 3C). To further evaluate whether lysosomal pH changes are responsible for the inhibitory effect of irinotecan on the autophagic flux, we carried out LC3 turnover assay as described by Mizushima *et al.*¹⁹ Incubation with the weak base CQ, which is known to block autophagy by elevating lysosomal pH, induced accumulation of LC3-II and p62 levels (figure 3D) and co-incubation with irinotecan did not induce a further accumulation of these markers (figure 3D). In contrast, re-acidifying of lysosomal pH using CLQ, a zinc ionophore, abolished the irinotecan mediated impairment of autophagy (figure 3D). Moreover, CLQ treatment significantly reduced irinotecan-induced steatosis of hepatocytes (figure 3E, F). Taken together, these results indicate that lysosomal alkalinising effects are responsible for the irinotecan-mediated block of autophagic flux and hepatic steatosis.

In vivo model of irinotecan-induced CASH

To verify our in vitro findings in vivo, irinotecan was applied to mice (50 mg/kg every three days) via intraperitoneal injections for 2 weeks. Control mice received solvent (saline) only. Under these experimental conditions, irinotecan caused only a slight

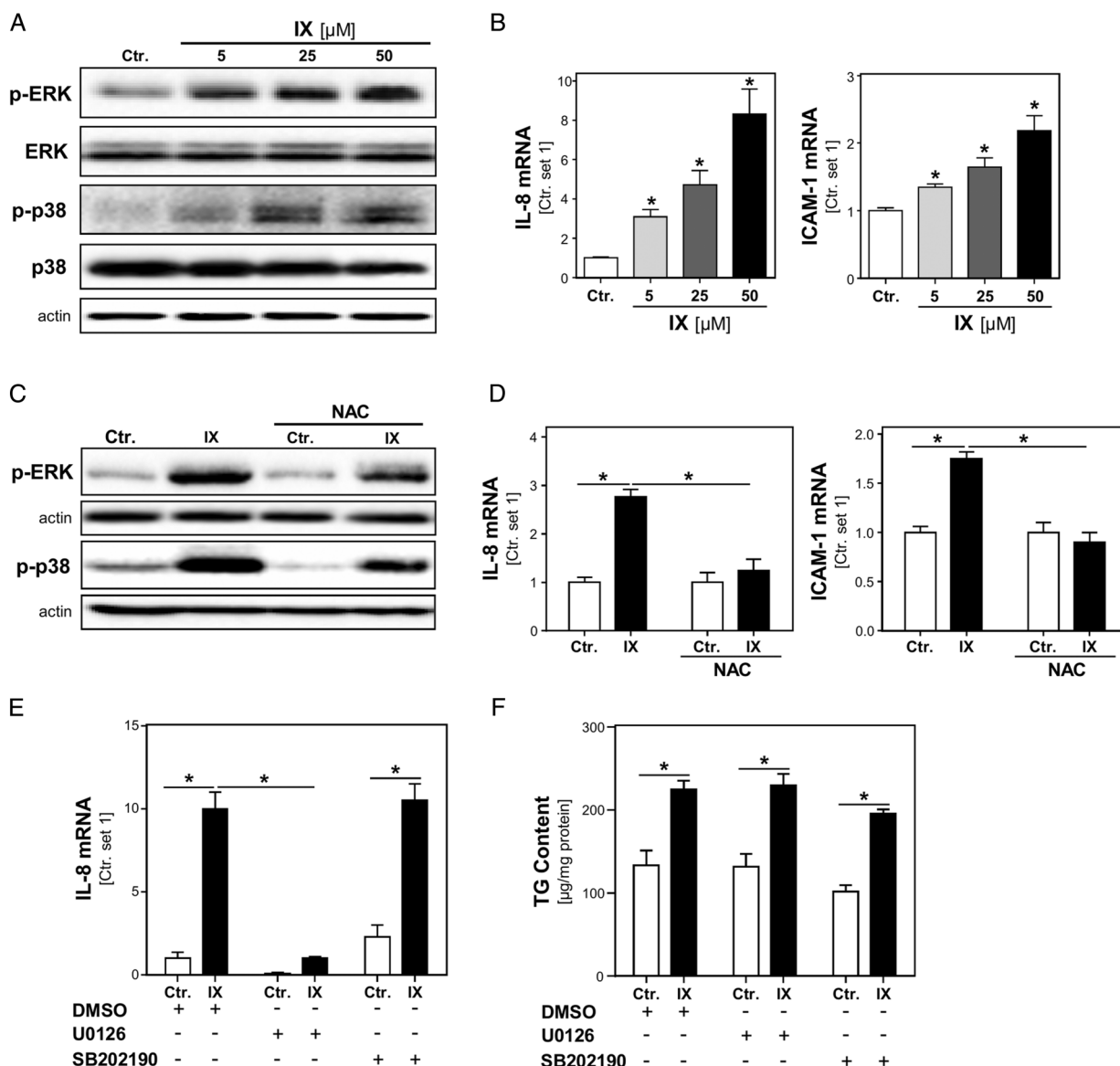


Figure 2 Effect of irinotecan (IX) on mitogen-activated protein kinase activation and pro-inflammatory gene expression in vitro. (A) Analysis of phosphorylated and unphosphorylated extracellular signal-regulated kinase (ERK) and p38 protein levels by western blot analysis in control hepatocytes (Ctr.) and cells treated with different IX doses as indicated. Actin served as control for loading adjustment. (B) Analysis of interleukin (IL)-8 and intercellular adhesion molecule 1 (ICAM-1) mRNA levels by quantitative reverse transcription PCR in IX-treated and control cells. (C) Analysis ERK and p38 phosphorylation in control (Ctr.) and IX-treated cells (25 μ M; 8 hours) with or without preincubation with N-acetylcysteine (NAC). (D) Analysis of IL-8 and ICAM-1 mRNA levels in control and IX-treated cells with and without NAC. (E) Analysis of IL-8 mRNA levels and (F) cellular triglyceride (TG) content in control and IX-treated cells (25 μ M) with or without preincubation with ERK inhibitor (U0126) or p38 inhibitor (SB202190) (* p <0.05).

increase of serum levels of transaminases (see online supplementary figure S3A). However, irinotecan-treated mice revealed significantly increased hepatic DGAT2 expression (figure 4A) as well as enhanced TG levels and microvesicular hepatic steatosis (figure 4B). Furthermore, CPT-1 expression was reduced (figure 4C) but ACOX1 expression and HMOX-1 expression as well as MDA levels were significantly higher in livers of irinotecan-treated mice compared with controls (figure 4C, D). Also, hepatic tumour necrosis factor (TNF)- α , IL-1 α , IL-1 β , c-x-c motif chemokine ligand 1 (CXCL1; GRO- α), ICAM-1, CCL5 and IL-6 expression were significantly induced by irinotecan treatment (figure 4E and online supplementary figure S3B). Also, CCL2 (MCP-1) expression was higher in irinotecan-treated mice but differences did not reach the level of

significance (see online supplementary figure S3B). Furthermore, immunohistochemical cluster of differentiation 3 (CD3) staining revealed a marked immune cell infiltration (figure 4F). In addition, irinotecan-induced hepatic steatosis and inflammation were accompanied by elevated levels of phosphorylated p38 and ERK proteins (figure 4G). An increased LC3-II/LC3-I ratio, together with an accumulation of p62 protein (figure 4G), was indicative of an impairment of autophagy in the livers of irinotecan-treated mice. Notably, a shift from CPT-1 to ACOX1 expression and a significant induction of hepatic steatosis and inflammatory response could already be observed in the livers of mice 24 hours after the application of a single irinotecan dose (see online supplementary figure S4A–E). Moreover, these changes were concomitant with an early impairment of

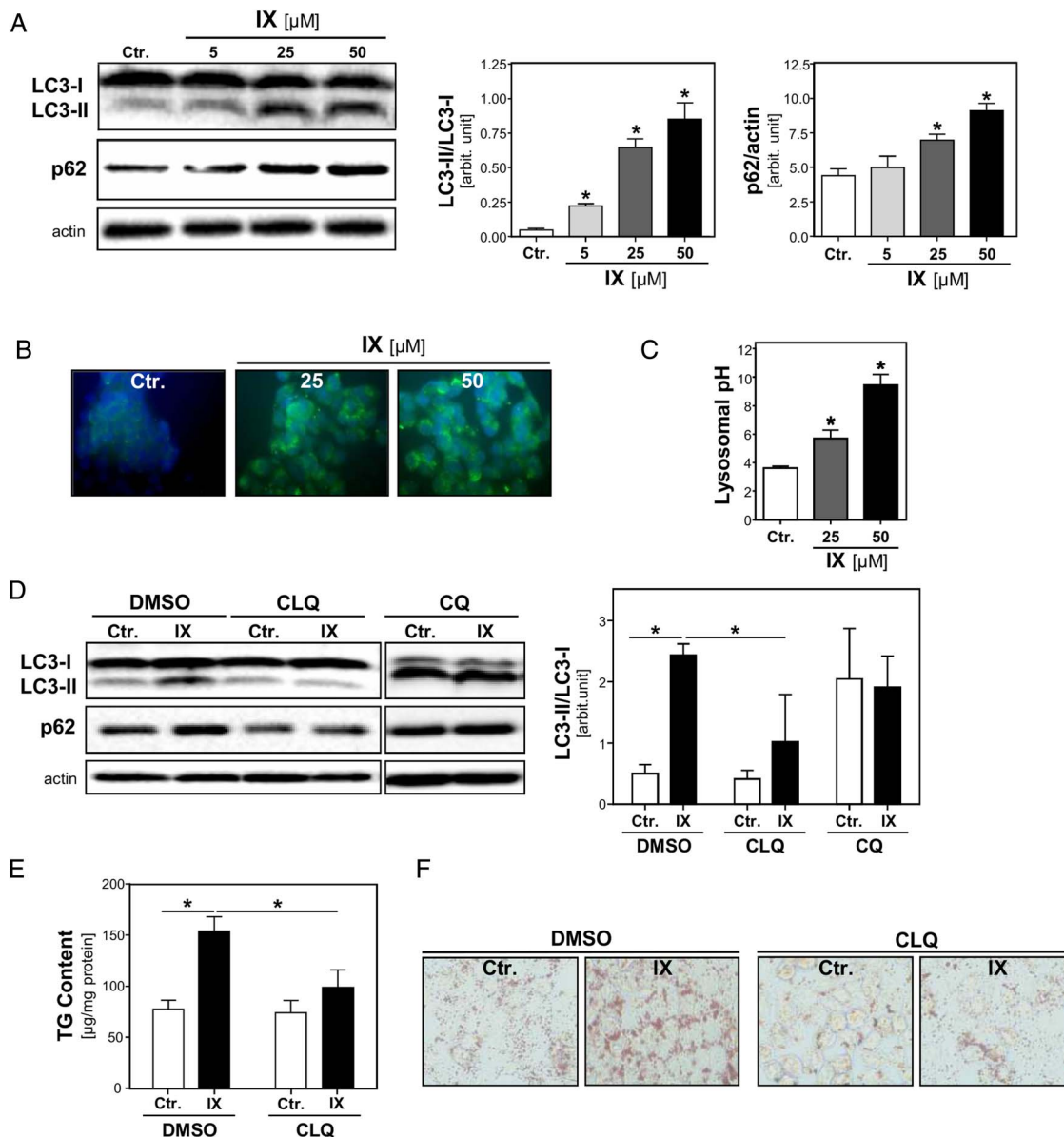


Figure 3 Effect of irinotecan (IX) on autophagy in vitro. (A) Analysis of light chain 3 (LC3) II/I and p62 protein levels by western blot analysis in control hepatocytes (Ctr.) and cells treated with different IX doses as indicated. Actin served as control for loading adjustment (left panel). Densitometric analysis of LC3II/I ratio (middle panel) and p62 levels (right panel). (B) Immunofluorescence analysis of LC3 and (C) analysis of lysosomal pH using ratiometric pH measurements with LysoSensor Yellow/Blue DND-160 in control cells and cell treated with 25 or 50 μM IX. (D) Analysis of LC3 II/I and p62 protein levels by western blot analysis in control cells and hepatocytes treated with IX (25 μM) in the presence or absence of chloroquine (CQ) or clioquinol (CLQ) (left panel); densitometric analysis of LC3II/I ratio (right panel). (E) Analysis of cellular triglycerides (TG) and (F) Microscopic images of Oil red O staining of control cells and hepatocytes treated with IX in the presence or absence of CLQ (* $p < 0.05$ compared with control).

autophagy as revealed by LC3 and p62 protein levels (see online supplementary figure S4F). In summary, the murine CASH model confirmed the in vitro data, indicating that oxidative stress-mediated MAPK activation and an impairment of hepatic autophagy are responsible for irinotecan-induced hepatic inflammation and steatosis.

Analysis of hepatic tissues from irinotecan-treated patients

To validate the experimental data, we analysed hepatic tissue specimens obtained from patients undergoing liver surgery for resection of hepatic metastases. Six patients had received irinotecan therapy and five patients had no chemotherapy prior to surgery. Despite the small number of samples, mRNA analyses

revealed significantly elevated DGAT2 (figure 5A) as well as ACOX1 and HMOX-1 (figure 5B) expression in livers of cancer patients pretreated with irinotecan. Furthermore, expression levels of several pro-inflammatory genes were significantly higher in irinotecan-treated patients compared with control patients (figure 5C and online supplementary figure S5). Also, the expression of ICAM-1 was increased but difference did not reach the level of significance (figure 5C). Moreover, irinotecan-treated patients revealed more hepatic ERK and p38 phosphorylation than controls (figure 5D, E). Also, LC3-II/LC3-I ratio and p62 protein levels were higher in liver tissue of irinotecan-treated patients although differences did not reach the level of significance (figure 5F). In summary, these findings confirm the

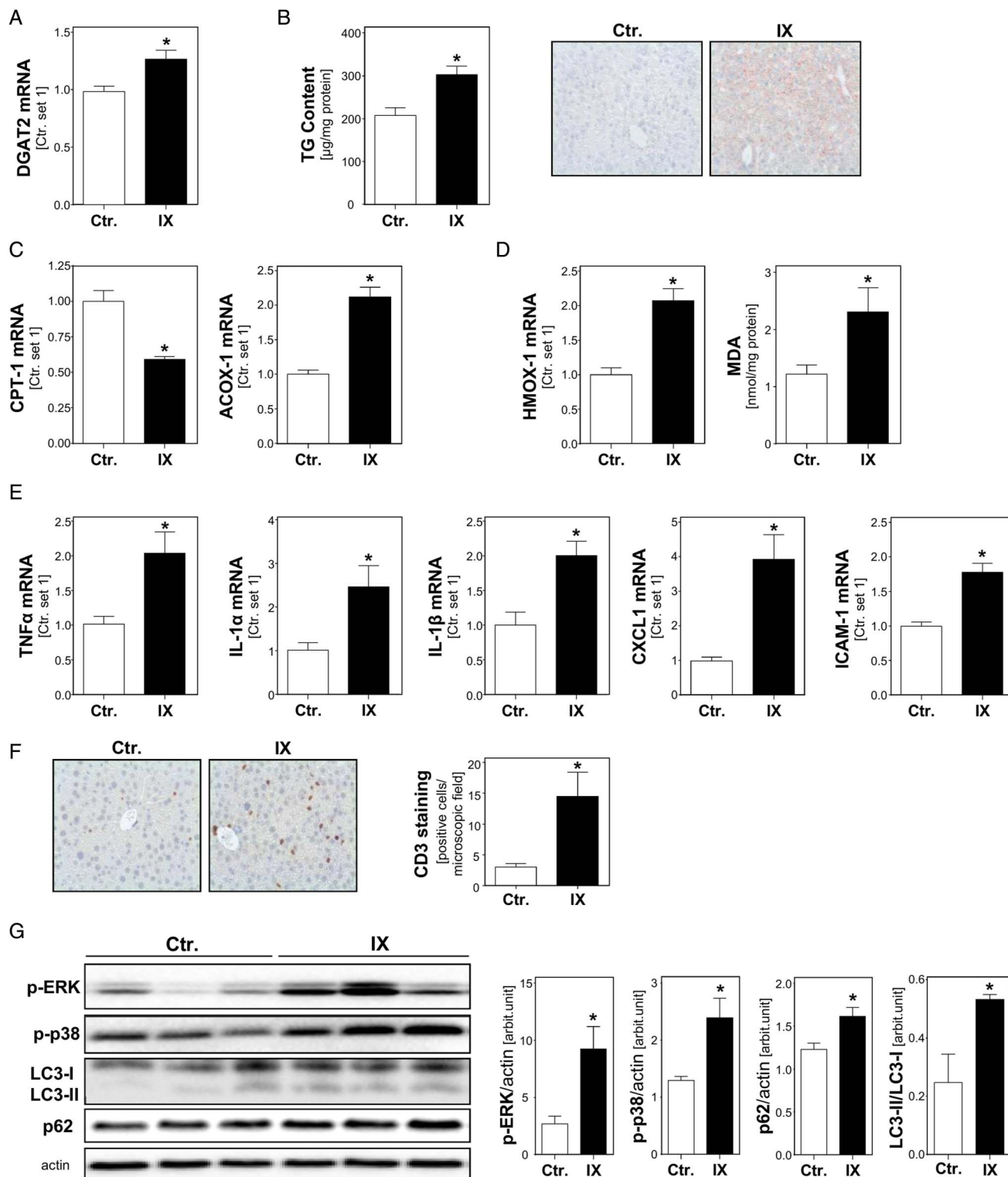


Figure 4 Irinotecan-induced steatohepatitis in vivo. Mice were treated with irinotecan (IX; 50 mg/kg intraperitoneally every three days for 2 weeks). Control mice (Ctr.) were injected with the solvent (saline). (A) Hepatic diglyceride acyltransferase 2 (DGAT2) mRNA levels analysed by quantitative real time-PCR. (B) Hepatic triglyceride (TG) content (left panel) and microscopic images of Sudan Red stained liver tissues (right panel). (C) Hepatic mRNA levels of carnitine palmitoyltransferase I (CPT-1) and acyl-coenzyme A oxidase-1 (ACOX-1). (D) Hepatic mRNA levels of haem oxygenase-1 (HMOX-1; left panel) and malondialdehyde (MDA) levels (right panel). (E) Hepatic mRNA levels of tumour necrosis factor (TNF)- α , interleukin (IL)-1 α , IL-1 β , c-x-c motif chemokine ligand 1 (CXCL1) and intercellular adhesion molecule 1 (ICAM-1). (F) Microscopic images of cluster of differentiation 3 (CD3) immunohistochemical staining of liver tissue (left panel) and quantification of CD3-stained cells (right panel). (G) Western blot analysis of phosphorylated extracellular signal-regulated kinase (ERK) and p38 as well as light chain 3 (LC3) I/II and p62 protein levels. Actin served as control for loading adjustment (left panel); densitometric analysis of the corresponding blots (right panel) (* $p < 0.05$ compared with control).

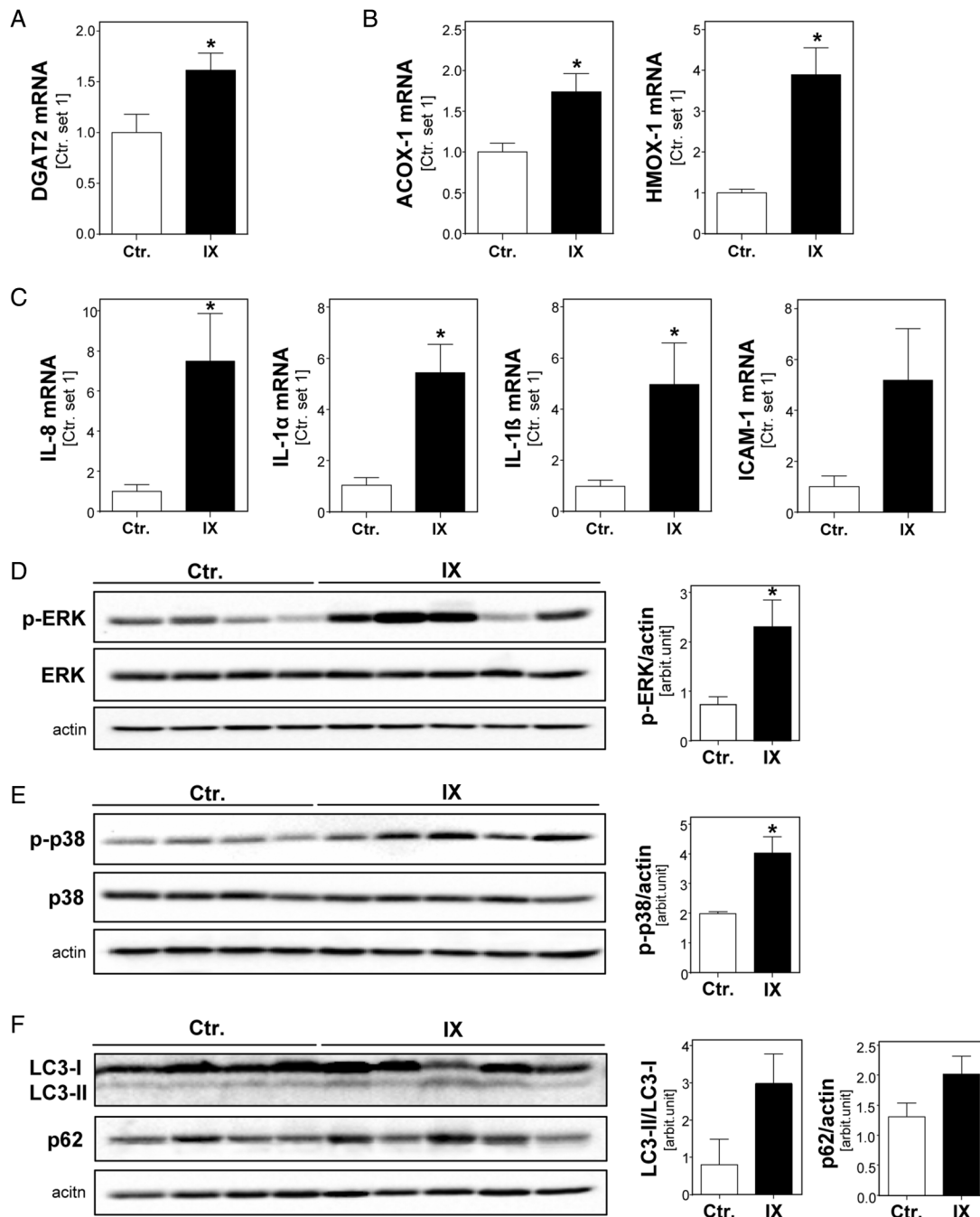


Figure 5 Hepatic mitogen-activated protein kinase activation, pro-inflammatory gene expression and autophagy in irinotecan (IX)-treated patients. Liver specimens of patients with metastatic colorectal cancer (i) with IX treatment (IX; n=6) or (ii) without chemotherapy (Ctr.; n=5) were analysed. Hepatic mRNA levels of (A) diglyceride acyltransferase 2 (DGAT2), (B) acyl-coenzyme A oxidase-1 (ACOX1) and haem oxygenase-1 (HMOX1), (C) interleukin (IL)-8, IL-1 α , IL-1 β and intercellular adhesion molecule 1 (ICAM-1) analysed by quantitative real time-PCR. Western blot analysis of phosphorylated and unphosphorylated (D) extracellular signal-regulated kinase (ERK) and (E) p38 protein levels. Actin served as control for loading adjustment (left panels); densitometric analysis of the corresponding blots (right panels). (F) Western blot analysis of light chain 3 (LC3) I/II and p62 protein levels. Actin served as control for loading adjustment (left panel); densitometric analysis (right panel) (* $p < 0.05$ compared with control).

data obtained in the in vitro and in vivo CASH models and suggest that in patients with cancer MAPK activation and impairment of the autophagic flux are the main pathological drivers of irinotecan-induced steatohepatitis.

Analysis of the effect of the tyrosine kinase inhibitor sorafenib on irinotecan-induced steatohepatitis

Recently, it has been reported that the multityrosine kinase inhibitor sorafenib induces autophagy and augments the

antitumour efficacy of irinotecan in hepatocellular carcinoma.^{20,21} This prompted us to analyse the effect of sorafenib in our experimental models of irinotecan-induced steatohepatitis. Pretreatment with sorafenib dose-dependently reduced irinotecan-induced ERK and p38 activation (figure 6A), and also IL-8 and ICAM-1 expression (figure 6B) in hepatocytes in vitro. At the highest concentration (4 μ M), irinotecan-induced MAPK activation and pro-inflammatory gene expression were completely blunted (figure 6A, B). In contrast, not even in a

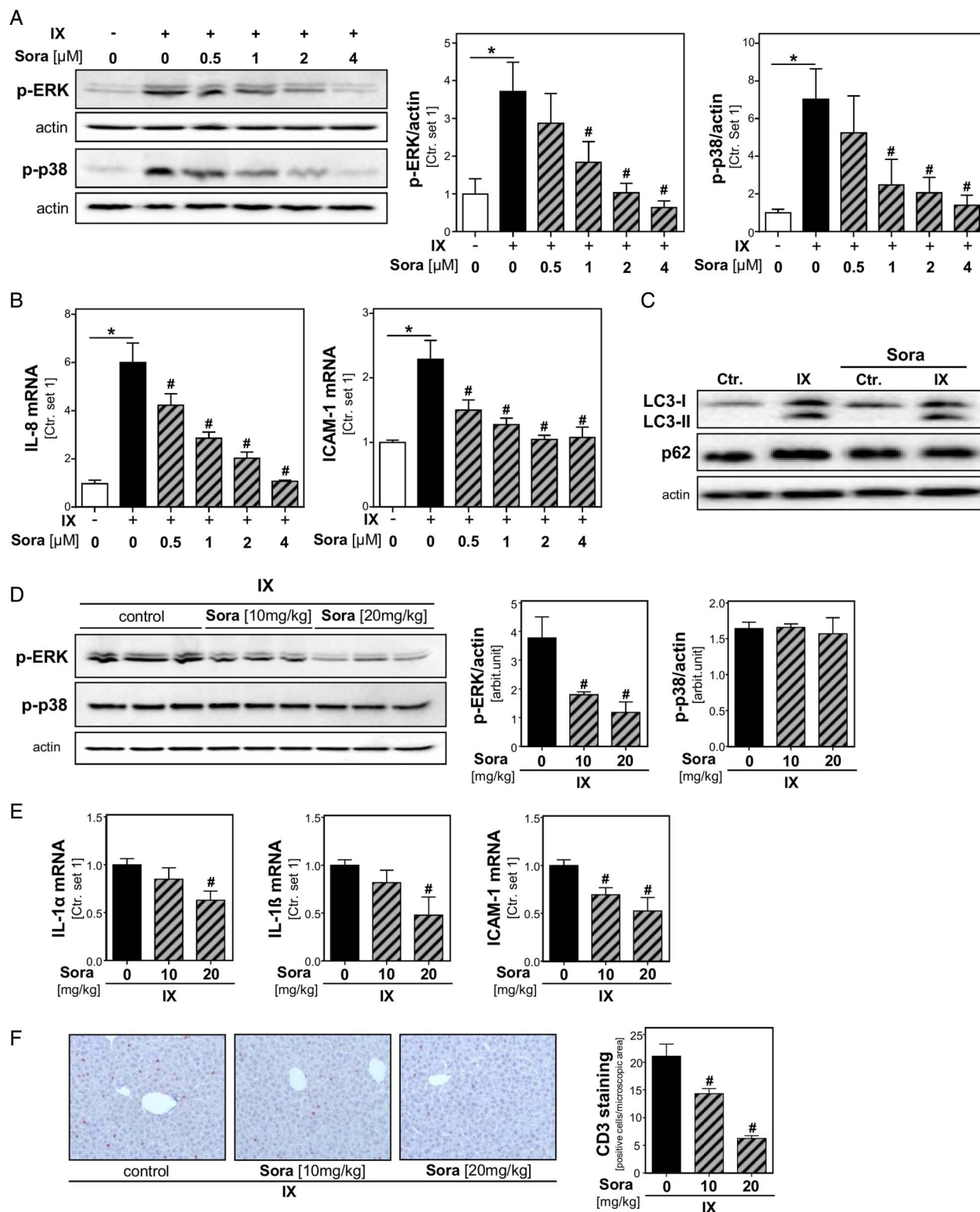


Figure 6 Effects of sorafenib (Sora) on irinotecan (IX)-induced steatohepatitis in vitro and in vivo. Hepatocytes were incubated with IX for 8 hours with or without pretreatment with different doses (0.5–4 μ M) of sorafenib (added 1 hour before IX). (A) Western blot analysis of phosphorylated p38 and extracellular signal-regulated kinase (ERK) protein levels. Actin served as control for loading adjustment (left panel); densitometric analysis (right panel). (B) Interleukin (IL)-8 and intercellular adhesion molecule 1 (ICAM-1) mRNA levels analysed by quantitative real time-PCR. (C) Western blot analysis of light chain 3 (LC3) II/I and p62 protein levels. Furthermore, mice were treated with sorafenib (10 or 20 mg/kg) 3 hours prior to application of a single IX dose (50 mg/kg). Control mice received solvent prior to IX injection (control group). Liver tissue was analysed 24 hours after IX application. (D) Western blot analysis p-ERK and p-38 protein levels (left panel); densitometric analysis (right panel). (E) IL-1 α , IL-1 β and ICAM-1 mRNA levels analysed by quantitative RT-PCR. (F) Microscopic images of cluster of differentiation 3 (CD3) immunohistochemical staining of liver tissues (left panel) and quantification of CD3-stained cells (right panel) (* p <0.05; # p <0.05 compared with only IX-treated group).

concentration of 4 μ M sorafenib significantly affected the irinotecan-mediated changes of the LC3-II/LC3-I ratio and p62 protein levels (figure 6C) or TG levels (see online supplementary figure S6A) in hepatocytes in vitro.

To analyse the effects of sorafenib in vivo, mice were pre-treated with two different doses of sorafenib (10 or 20 mg/kg) 3 hours prior to the application of irinotecan (50 mg/kg). Control mice received solvent only. After 24 hours, hepatic tissues from both sorafenib co-treated mice groups showed significantly lower ERK phosphorylation compared with mice that received only irinotecan (figure 6D). Furthermore, IL-1 α , IL-1 β and ICAM-1 expression were significantly lower in mice pre-treated with the high (20 mg/kg) sorafenib dose (figure 6E). Also, mice pretreated with the low (10 mg/kg) sorafenib dose revealed reduced pro-inflammatory gene expression but in this group only for ICAM-1 differences reached the level of significance compared with control mice (figure 6E). Moreover, sorafenib treatment caused a dose-dependent reduction of irinotecan-induced hepatic immune cell infiltration (figure 6F). In contrast, not even the high sorafenib dose (20 mg/kg) significantly affected irinotecan-mediated changes of hepatic p38 activation (figure 6D), LC3-II/LC3-I ratio, p62 protein levels and lipid levels (see online supplementary figure S6B–D). In summary, these results indicate that a combination of irinotecan

and sorafenib does not only exert a chemosensitising effect on cancer cells but also a protective effect on irinotecan-induced inflammation in non-cancerous liver tissue.

DISCUSSION

The aim of this study was to investigate the molecular mechanisms by which irinotecan induces hepatic steatosis and inflammation. Previous studies demonstrated that irinotecan is toxic to hepatocytes in a dose-dependent manner.²² Hepatocyte destruction may be responsible for acute hepatic drug toxicity; however, it cannot explain the typical findings of steatohepatitis. Therefore, we applied irinotecan in doses not leading to significant hepatocellular injury. Under these experimental conditions, irinotecan induced oxidative stress-mediated MAPK activation and pro-inflammatory gene expression in hepatocytes and murine livers. As likely reason for the irinotecan-induced oxidative stress response, we identified an impairment of mitochondrial function. Irinotecan is a precursor of the lipophilic metabolite SN-38, and it has been shown for other drugs that cause steatohepatitis, such as amiodarone and tamoxifen, that agents with lipophilic moieties cross the mitochondrial membrane and inhibit mitochondrial oxidation and electron transfer along the respiratory chain, resulting in production of ROS.²³ A further consequence of impaired mitochondrial β -oxidation is a

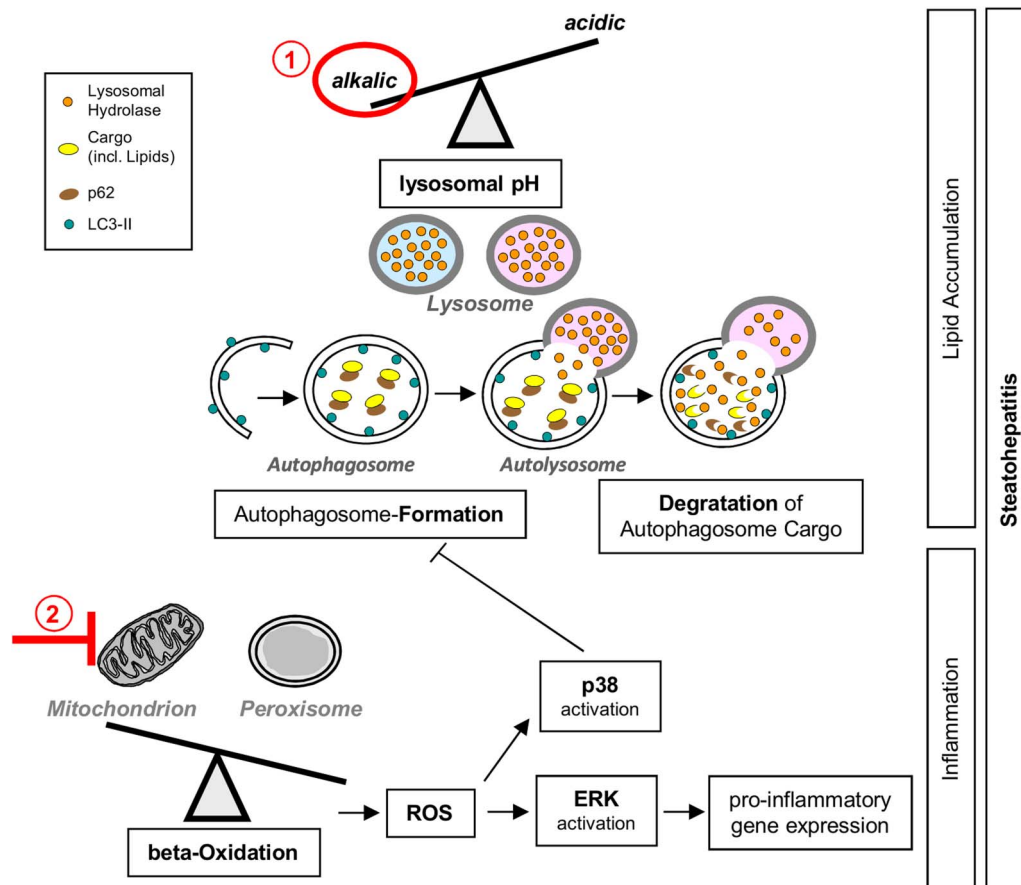


Figure 7 Model of molecular mechanism of irinotecan-induced steatohepatitis. Irinotecan-induced hepatocellular lipid accumulation and inflammation are mediated via impairment of different cellular organelles and mechanisms, respectively. ① Irinotecan alkalises the lysosomal pH and herewith impairs the autophagic flux, which causes cellular lipid accumulation and steatosis. ② Irinotecan impairs the mitochondrial function and herewith causes a shift from mitochondrial towards peroxisomal β -oxidation. This causes an enhanced formation of reactive oxygen species (ROS) and subsequently an activation of mitogen-activated protein kinases extracellular signal-regulated kinase (ERK) and p38. ERK activation causes pro-inflammatory gene expression and inflammation. Although not analysed in more detail in this study, induction of p38 is known as inhibitor of autophagosome formation, and thus, possibly further contributes to irinotecan-induced lipid accumulation. LC3, light chain 3.

shift to extra-mitochondrial pathways. In line with this, we observed a significant upregulation of ACOX1, the initial enzyme for peroxisomal β -oxidation, in irinotecan-treated hepatocytes and in murine and human liver tissues. This form of fatty acid combustion causes increased hydrogen peroxide generation and thus contributes to harmful ROS production in addition to an impaired respiratory chain.

While ROS scavenging almost completely inhibited irinotecan-induced ERK and p38 activation and pro-inflammatory gene expression, it did not affect hepatocellular steatosis. Instead, we identified an impairment of the autophagic flux as the cause of lipid accumulation in hepatocytes. As underlying mechanisms, we discovered lysosomal alkalinising effects of irinotecan. The structure of irinotecan contains four nitrogen atoms, which makes its solution alkaline. Weak bases can be protonated and can accumulate in lysosomes, resulting in the deacidification of their lumen.^{24–25} The lumen of the lysosome contains approximately 60 types of soluble hydrolases.¹⁸ These enzymes are active in acidic environments and, as such, are responsible for the lysosomal hydrolysis of different substrates, including the cargo of autophagosomes.¹⁸ The MAPK p38 inhibits autophagy already at the level of autophagosome growth by competing with transmembrane protein mAtg9 for binding to p38 interacting protein.²⁶ This explains why inhibition of irinotecan-induced p38 activation did not affect hepatocellular steatosis. Also, ERK inhibition did not affect irinotecan-induced steatosis but appeared to be the critical mediator of irinotecan-induced pro-inflammatory gene expression in hepatocytes. Figure 7 provides a diagrammatic sketch depicting the molecular mechanism of irinotecan causing hepatic lipid accumulation and pro-inflammatory gene expression.

Similarly to the specific ERK inhibitor U0126, sorafenib significantly reduced irinotecan-induced ERK activation and pro-inflammatory gene expression in hepatocytes in vitro and murine livers in vivo. Previous experimental studies indicated the potential of this multityrosine kinase inhibitor to augment the antitumour efficacy of irinotecan in hepatocellular carcinoma cells^{20–21} and to overcome irinotecan resistance in colorectal cancer cells in mice.²⁷ Furthermore, the Web-based register ClinicalTrials.gov (<https://clinicaltrials.gov>) specifies ongoing and recently closed studies, respectively, analysing the safety and efficacy of a combined therapy with irinotecan and sorafenib versus irinotecan or sorafenib monotherapy in patients with colorectal neoplasms or paediatric solid tumours. Until now it is mainly thought that the combinatory therapy with sorafenib and irinotecan can augment antitumour efficacy and overcome irinotecan resistance. Our study newly indicates that a combined application of sorafenib and irinotecan is also a promising option for the prevention of irinotecan-induced (steato)hepatitis and here-with discovers a potential new medical indication for this multityrosine kinase inhibitor. Still, future studies are warranted to confirm this sorafenib effect in irinotecan-treated patients and to investigate the optimal doses of the sorafenib-irinotecan combination in the therapeutic management of patients with colorectal cancer and other tumour entities. Indeed, previous studies have shown that sorafenib can exhibit (hepato)toxic effect in higher doses in mice²⁸ and men.²⁹ Furthermore, the potential of targeting lysosomal pH for the prevention and treatment of irinotecan-induced steatohepatitis needs to be explored. In this study, we developed valid in vitro and in vivo models that can be the basis for further preclinical investigations.

Acknowledgements The authors thank Birgitta Ott-Rötzer, Heidi Gschwendtner and Rudolf Jung for excellent technical assistance. They also acknowledge the

Human Tissue and Cell Research (HTCR) Foundation for making human tissue available for research and Hepacult GmbH (Regensburg, Germany) for providing primary human hepatocytes for in vitro studies. The authors also appreciate the complex data and sample analysis of the Biobank o.b. HTCR of the Ludwig-Maximilians-University Munich to provide the selected liver tissue samples.

Contributors AM, MS, AK, JS and PD performed the experiments. AM, JS-L, AL, AK and CH analysed the data. SL, RT, WET, MM and AKB provided material and performed Biobank search and analyses. AM and CH designed the project and wrote the manuscript.

Funding This work was supported by grants from the German Research Association (DFG) to AB and CH (FOR 2127; Bo1573 and He2458) and CH (KFO262; He2458) and by the Interdisciplinary Center for Clinical Research (IZKF) Erlangen to PD (J55) and AB (D24).

Competing interests None declared.

Ethics approval Tissue and Cell Research (HTCR) Foundation.

Provenance and peer review Not commissioned; externally peer reviewed.

REFERENCES

- Khan AZ, Morris-Stiff G, Makuuchi M. Patterns of chemotherapy-induced hepatic injury and their implications for patients undergoing liver resection for colorectal liver metastases. *J Hepatobiliary Pancreat Surg* 2009;16:137–44.
- Chun YS, Laurent A, Maru D, et al. Management of chemotherapy-associated hepatotoxicity in colorectal liver metastases. *Lancet Oncol* 2009;10:278–86.
- Morris-Stiff G, Tan YM, Vauthey JN. Hepatic complications following preoperative chemotherapy with oxaliplatin or irinotecan for hepatic colorectal metastases. *Eur J Surg Oncol* 2008;34:609–14.
- Robinson SM, Wilson CH, Burt AD, et al. Chemotherapy-associated liver injury in patients with colorectal liver metastases: a systematic review and meta-analysis. *Ann Surg Oncol* 2012;19:4287–99.
- Zorzi D, Laurent A, Pawlik TM, et al. Chemotherapy-associated hepatotoxicity and surgery for colorectal liver metastases. *Br J Surg* 2007;94:274–86.
- Lee SM, Schelcher C, Laubender RP, et al. An algorithm that predicts the viability and the yield of human hepatocytes isolated from remnant liver pieces obtained from liver resections. *PLoS ONE* 2014;9:e107567.
- Lee SM, Schelcher C, Demmel M, et al. Isolation of human hepatocytes by a two-step collagenase perfusion procedure. *J Vis Exp* 2013. doi:10.3791/50615
- Messerer CL, Ramsay EC, Waterhouse D, et al. Liposomal irinotecan: formulation development and therapeutic assessment in murine xenograft models of colorectal cancer. *Clin Cancer Res* 2004;10:6638–49.
- Thasler WE, Weiss TS, Schillhorn K, et al. Charitable state-controlled foundation human tissue and cell research: ethic and legal aspects in the supply of surgically removed human tissue for research in the academic and commercial sector in Germany. *Cell Tissue Bank* 2003;4:49–56.
- Varanasi U, Chu R, Chu S, et al. Isolation of the human peroxisomal acyl-CoA oxidase gene: organization, promoter analysis, and chromosomal localization. *Proc Natl Acad Sci USA* 1994;91:3107–11.
- Braunersreuther V, Viviani GL, Mach F, et al. Role of cytokines and chemokines in non-alcoholic fatty liver disease. *World J Gastroenterol* 2012;18:727–35.
- Ito S, Yukawa T, Uetake S, et al. Serum intercellular adhesion molecule-1 in patients with nonalcoholic steatohepatitis: comparison with alcoholic hepatitis. *Alcohol Clin Exp Res* 2007;31:S83–7.
- Li BH, He FP, Yang X, et al. Steatosis induced CCL5 contributes to early-stage liver fibrosis in nonalcoholic fatty liver disease progress. *Transl Res* 2016. doi:10.1016/j.trsl.2016.08.006. [Epub ahead of print 31 Aug 2016].
- Corcelle E, Djerbi N, Mari M, et al. Control of the autophagy maturation step by the MAPK ERK and p38: lessons from environmental carcinogens. *Autophagy* 2014;3:57–9.
- Wu D, Cederbaum AI. Inhibition of autophagy promotes CYP2E1-dependent toxicity in HepG2 cells via elevated oxidative stress, mitochondrial dysfunction and activation of p38 and JNK MAPK. *Redox Biol* 2013;1:552–65.
- Ding WX, Li M, Chen X, et al. Autophagy reduces acute ethanol-induced hepatotoxicity and steatosis in mice. *Gastroenterology* 2010;139:1740–52.
- Dong H, Czaja MJ. Regulation of lipid droplets by autophagy. *Trends Endocrinol Metab* 2011;22:234–40.
- Settembre C, Fraldi A, Medina DL, et al. Signals from the lysosome: a control centre for cellular clearance and energy metabolism. *Nat Rev Mol Cell Biol* 2013;14:283–96.
- Mizushima N, Yoshimori T, Levine B. Methods in mammalian autophagy research. *Cell* 2010;140:313–26.
- Wang Z, Zhao Z, Wu T, et al. Sorafenib-irinotecan sequential therapy augmented the anti-tumor efficacy of monotherapy in hepatocellular carcinoma cells HepG2. *Neoplasia* 2015;62:172–9.
- Shi YH, Ding ZB, Zhou J, et al. Targeting autophagy enhances sorafenib lethality for hepatocellular carcinoma via ER stress-related apoptosis. *Autophagy* 2011;7:1159–72.

- 22 Zhou S, Li N, Wang X, *et al.* In vitro cytotoxicity, pharmacokinetics and tissue distribution in rats of MXN-004, a novel conjugate of polyethylene glycol and SN38. *Xenobiotica* 2014;44:562–9.
- 23 Pessayre D, Berson A, Fromenty B, *et al.* Mitochondria in steatohepatitis. *Sem Liver Dis* 2001;21:57–69.
- 24 Kimura T, Takabatake Y, Takahashi A, *et al.* Chloroquine in cancer therapy: a double-edged sword of autophagy. *Cancer Res* 2013;73: 3–7.
- 25 Homewood CA, Warhurst DC, Peters W, *et al.* Lysosomes, pH and the anti-malarial action of chloroquine. *Nature* 1972;235:50–2.
- 26 Webber JL, Tooze SA. Coordinated regulation of autophagy by p38alpha MAPK through mAtg9 and p38IP. *EMBO J* 2010;29:27–40.
- 27 Mazard T, Causse A, Simony J, *et al.* Sorafenib overcomes irinotecan resistance in colorectal cancer by inhibiting the ABCG2 drug-efflux pump. *Mol Cancer Ther* 2013;12:2121–34.
- 28 Tang TC, Man S, Xu P, *et al.* Development of a resistance-like phenotype to sorafenib by human hepatocellular carcinoma cells is reversible and can be delayed by metronomic UFT chemotherapy. *Neoplasia* 2010;12:928–40.
- 29 Van Hootegem A, Verslype C, Van Steenberghe W. Sorafenib-induced liver failure: a case report and review of the literature. *Case Rep Hepatol* 2011;2011:941395.